



Stochastic annealing simulation of intracascade defect interactions

H.L. Heinisch ^{a,*}, B.N. Singh ^b

^a *Materials and Chemical Sciences Department, Pacific Northwest National Laboratory ¹, P Box 999 Richland, WA 99352, USA*

^b *Materials Research Department, Risø National Laboratory, 4000 Roskilde, Denmark*

Abstract

Atomic scale computer simulations are used to investigate the intracascade evolution of the defect populations produced in cascades in copper over macroscopic time scales. Starting with cascades generated using molecular dynamics, the diffusive transport and interactions of the defects are followed for hundreds of seconds in stochastic annealing simulations. The temperature dependencies of annihilation, clustering and free defect production are determined for individual cascades, especially including the effects of the subcascade structure of high energy cascades. The subcascade structure is simulated by closely spaced groups of lower energy MD cascades. The simulation results illustrate the strong influence of the defect configuration existing in the primary damage state on subsequent intracascade evolution. Other significant factors affecting the evolution of the defect distribution are the large differences in mobility and stability of vacancy and interstitial defects and the rapid one-dimensional diffusion of small, glissile interstitial clusters produced directly in cascades. Annealing simulations are also performed on high-energy, subcascade-producing cascades generated with the binary collision approximation and calibrated to MD results. © 1997 Elsevier Science B.V.

1. Introduction

It is well established that clusters of both vacancies and self-interstitial atoms (SIAs) can form directly in displacement cascades, depending on the material and the cascade energy. Once formed, the clusters can migrate (climb and glide), shrink by recombination, grow by absorption and coalescence and dissolve by thermal dissociation, depending on the irradiation temperature. To understand these processes and their impact on defect accumulation, which occur over time and size scales spanning many orders of magnitude, it is necessary to invoke a suite of models. Each model must describe the relevant phenomena within the time and size scales to which it applies, as well as smoothly interfacing with the other models. At the atomic scale, molecular dynamics (MD) simulations can be used to describe the earliest stages of defect production in cascades. Reaction rate theories apply to the global distri-

bution and interactions of defects over macroscopic distances and times. However, the time and distance scales of MD and rate theory do not overlap. Even after the longest practical MD simulation, the defect clusters of a single cascade remain spatially localized in a 'metastable' state far from the spatial and temporal uniformity required for the global picture to which a rate theory approach may be applied. Atomic scale stochastic annealing simulation provides the necessary link between the localized, short-term, atomistic view of individual MD cascades and the spatially averaged global view required for the application of rate theory.

Besides the annealing stage of a single, isolated cascade, there are a number of other physical aspects of defect evolution under cascade-producing irradiation that must be considered at the atomic scale and are most realistically addressed through a combination of MD, annealing simulations and other special considerations. These include the interaction of defects from cascades or subcascades produced concurrently in close proximity, the interaction of defects from a new cascade with debris (remaining defects) of a previous cascade or other elements of the existing microstructure, and the global evolution of the cluster distribution under irradiation during the transient

* Corresponding author. Tel.: +1-509 376 3278; fax: +1-509 376 0418; e-mail: hl_heinisch@pnl.gov.

¹ Pacific Northwest National Laboratory is operated for the US Department of Energy by Battelle Memorial Institute under contract DE-AC06-76RLO 1830.

period. A significant limitation of this multi-model, atomic-scale approach is that high-energy, subcascade-producing cascades are well beyond the practical size limit of MD simulations.

In this paper we will briefly discuss the models of defect accumulation and evolution and then illustrate the significant influence of initial defect clustering within cascades on the subsequent behavior of the defects. We will then address the interaction of defects within a group of subcascades, studied by stochastic annealing simulations on multiple MD cascades in close proximity. Preliminary results of annealing simulations of high-energy, subcascade-producing cascades generated with the binary collision approximation and calibrated to MD results will be examined. The paper concludes with a discussion of the annealing simulations reported here and their relationship to outstanding issues in the production and accumulation of defects.

2. Models of defect accumulation and evolution

Over the years, numerous attempts have been made to describe the microstructure evolution and defect accumulation using the mean field theory and reaction rate equations. These treatments do not consider the consequences of intracascade clustering of SIAs (see Ref. [1] for a recent review) on the magnitude and the kinetics of defect accumulation under cascade damage conditions, where the defect production is not homogeneous in space nor in time. The consequences of intracascade clustering of SIAs and vacancies, and of the thermal stability of these clusters, have been specifically addressed in the recently proposed 'production bias model' (PBM) [2,3]. The PBM has been further developed to account for the very important consequences of one-dimensional transport of small, glissile SIA clusters [4–6] and of the continuous transformation of sessile SIA clusters into glissile ones due to their interactions with single vacancies [7].

The PBM or any other such model can predict the global behavior of the system over macroscopic sizes and times. However, it has the limitation of not being able to deal explicitly with the problem of temporal and spatial fluctuations in the defect cluster production and size distributions occurring continuously under cascade damage conditions. At present, these cascade phenomena are dealt with by assuming some global average values for the relevant parameters. Clearly, accurate and reliable predictions from the PBM or other such models are possible only if physically realistic values for their input parameters can be obtained either experimentally (unlikely) or from atomic-scale models that include explicit temporal and spatial information. The determination of parameters for PBM from results of these models is, therefore, of crucial importance.

Annealing simulations, which stochastically model de-

fect diffusion, dissociation and interaction, can be used to follow the evolution of defect clusters within the cascade region beyond the metastable configuration remaining after MD simulations. Applied to the 'annealing stage' of individual cascades, its results can provide a defect production source term of potential use in rate theory descriptions of the global defect evolution. On the other hand, knowing the local defect configuration in the cascade region after the local, short-term annealing stage, as well as the numbers of defects that escape the cascade region during annealing, may not be enough to provide correct source information for rate theories. It may be necessary to incorporate additional information on averaging over the spatial and temporal inhomogeneity of cascade production into the rate theories. Such information could be obtained from stochastic annealing models of defect accumulation in a representative volume under continuous irradiation.

3. The stochastic annealing model

The stochastic annealing methods used here are often referred to as 'Monte Carlo annealing' or 'kinetic Monte Carlo' methods. We prefer to use the term 'stochastic annealing simulation' to emphasize the totally random processes by which the defect transport and interactions are simulated in the annealing model, to differentiate it from the deterministic particle interactions in binary collision and MD simulations used in various 'Monte Carlo' applications. Because the annealing simulation itself is stochastic and the variability of cascade configurations is so great, the annealing simulations are done in great numbers and average behavior is reported.

It is clear that the evolution of an individual cascade must continue to be followed on the atomic scale beyond the first 100 ps, until the localized concentration of cascade defects and its cascade nature has dissipated and the defects can properly be considered as part of the global defect distribution. The need to address this 'short-term annealing' stage of the cascade evolution on an atomic scale was recognized as early as the 1960s [8,9]. Annealing simulation models were developed then, in advance of the first MD cascade simulations, using binary collision cascades as input. Although the binary collision model provides a good description of the collisional stage of the cascade, considerable recombination, clustering and rearrangement of the defects takes place during the development and quenching of the thermal spike, i.e., before the annealing stage. Thus, in those early annealing simulations, the binary collision cascades had far too many 'defects' to start with, and these defects were not in realistic equilibrium positions (they were actually energetic displaced atoms, not stable point defects). Later annealing simulations using binary collision cascades [10] applied a semi-empirical quenching model, based on simple recombination, to the cascades before annealing to account for

some of these effects. Recently, with the availability of cascades of relatively high energy simulated through the quenching stage by MD, the stochastic annealing simulation concept has been revived as the primary focus of a multi-model approach to cascade defect evolution [11–13].

The stochastic annealing simulation code ALSOME was used for the studies on copper reported here. The annealing model and the ALSOME code, especially the selection of input parameters, are described in greater detail elsewhere [14]. Relative jump frequencies for all mobile defects, including mobile clusters, are determined from migration energies of defects in copper that are obtained largely from calculations. The same model and input parameter values used in Ref. [14] were employed in the present studies except where noted.

In the present model for copper, as in earlier annealing simulations, SIA clusters containing from one to three interstitials, and vacancy clusters containing from one to four vacancies, are assumed to migrate three-dimensionally with activation energies on the order of those for single SIAs and vacancies, respectively. A recently added feature of the annealing model is that somewhat larger SIA clusters are also allowed to move by gliding one dimensionally with a low migration energy. Molecular dynamics simulations indicate that SIA clusters form directly in cascades and collapse to glissile loops that migrate significant distances in one dimension with about the same activation energy as single SIAs [4,5]. In Ref. [14] all SIA clusters containing from four to nine interstitial atoms were assumed to be in the form of glissile loops that glide one-dimensionally with a migration energy of 0.1 eV. This model of glissile SIA clusters is based on analysis by Trinkaus et al. [4,5] of results of MD cascade simulations.

In the earlier work [14] two isolated individual 25 keV cascades in copper generated by MD [15] were annealed at various temperatures up to 550 K, for a simulated time about equal to the time between cascades in the annealing volume during a typical reactor irradiation. The temperature dependence of surviving and escaping defect fractions are shown in Fig. 1. The fractions of surviving defect pairs (the vacancy–interstitial pairs, both within the cascade region and outside it, that did not recombine within the region) and escaping vacancies and SIAs (those that migrated out of the cascade annealing volume) are reported relative to the number of defects at the beginning of the annealing simulation, which is after the quenching of the thermal spike (the end of the MD calculations). These results show that during the annealing stage up to 20% of the initial pairs recombine, depending on the temperature. The fraction of interstitial defects (measured in terms of individual point defects) that escapes the cascade region in Fig. 1 has weak sensitivity to temperature above 50 K, showing only small responses to increases in the mobile vacancy population. It is important to note that about 60% of the escaping SIAs are in the form of small clusters, containing 4–9 SIAs, gliding one-dimensionally, while the

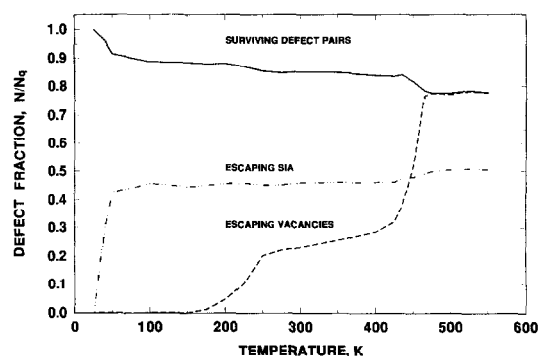


Fig. 1. The fractions of point defects surviving recombination and of vacancies and interstitials escaping from 25 keV cascades in copper during the annealing stage, as a function of cascade annealing temperature. The average of 100 anneals of each of two 25 keV cascades in copper generated in MD simulations is plotted. The defect fractions are relative to the total number of point defects at the end of the quench stage.

remainder have 1–3 SIAs and migrate three-dimensionally. Vacancies escape only above about 150 K, and no vacancies remain in the cascade region above about 450 K, where all vacancy clusters are quite unstable to thermal dissolution. According to this model, at temperatures above 50 K, 30–40% of the initial SIAs will remain in the cascade region as sessile clusters, while 0–90% of the vacancies will remain in the cascade region, depending on the temperature.

4. Interactions of defects from adjacent subcascades

Irradiations by high energy sources such as fusion neutrons, spallation neutrons, high energy protons and heavy ions produce a significant amount of damage in the form of high energy cascades that have multiple subcascades. It is important to know how the defect evolution within the high energy cascade is affected by the presence of subcascades in close proximity. Present computational resources are not capable of routinely generating high energy cascades by MD in the large numbers and arbitrary orientations required for good statistics (the highest energy MD cascades at present are several 40 keV cascades in iron that do show significant subcascade structure [16]). Even MD simulations of higher energy cascades with single damage regions (15–25 keV in copper or iron) are few in number. The two 25 keV cascades referred to in Fig. 1 are the highest energy MD cascades in copper. However, it should be possible to study the effects of subcascades on the annealing stage of high energy cascades by simply ‘constructing’ multiple-subcascade cascades from a set of lower energy cascades, i.e., by placing individual cascades in close proximity and annealing them simultaneously. This procedure does not, of course, ad-

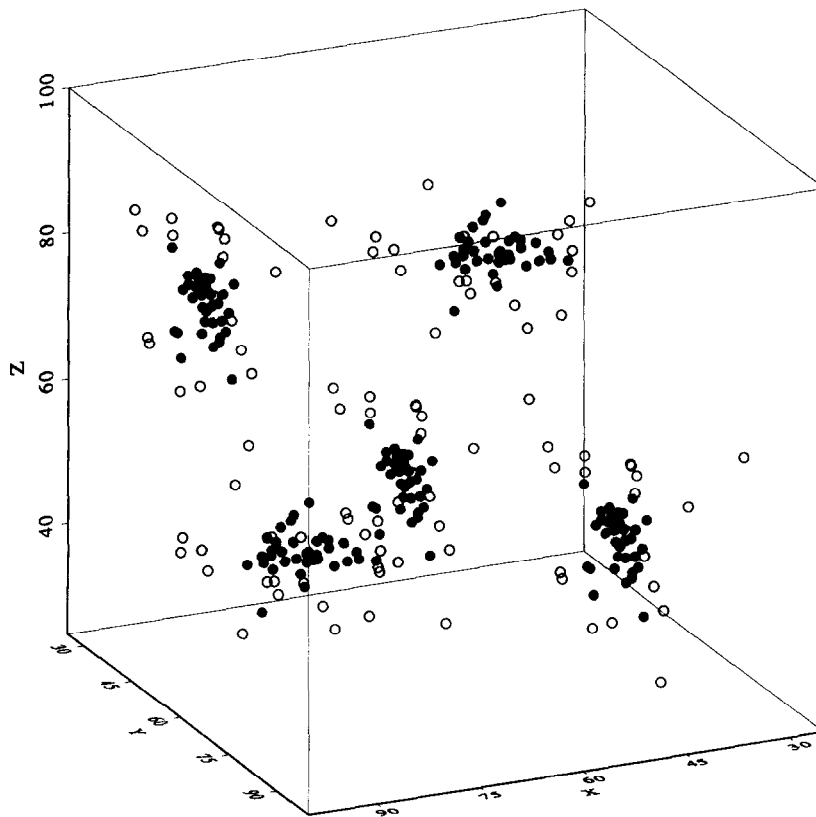


Fig. 2. A 'pseudo-' high energy cascade in copper. Each of the five 'subcascades' is a quenched 25 keV cascade from MD simulations, placed at random within 35 lattice parameters center-to-center of each other. The cascades are slightly closer together on average than the average subcascade spacing in copper. The filled circles represent vacancies and the open circles depict the SIAs. The scale on the enclosing box is in lattice parameters.

dress the possible interactions among subcascades during the thermal spike or quenching stages.

Multiple-subcascade cascades in copper were approximated by replicating the two 25 keV copper cascades above in several randomly chosen positions at a fixed separation distance to produce cascades with 2–5 'subcascades'. Fig. 2 illustrates a pseudo-cascade with five subcascades constructed from the two 25 keV cascades. The center-to-center separation of the subcascades was set to 35 lattice parameters, slightly less than the average subcascade spacing determined in binary collision simulations of copper cascades [17]. The pseudo-cascades were also given a more compact configuration, with every subcascade in close proximity to as many others as possible compared to the average cascade in copper, to maximize possible effects of intersubcascade defect interactions. Anneals were performed on 100 such pseudo-cascades at 400 K as a function of the number of subcascades in a group. At this temperature significant fractions of both vacancies and SIAs are mobile. The results are shown in Fig. 3. The intersubcascade defect interactions are minimal, as demonstrated by only a small systematic decrease in surviving

and escaping defect fractions as the number of subcascades per cascade increases. At other annealing temperatures (Fig. 4), there is little effect of close subcascade proximity for groups of five subcascades. The fractions of surviving pairs and escaping defects are about 10% less than for the

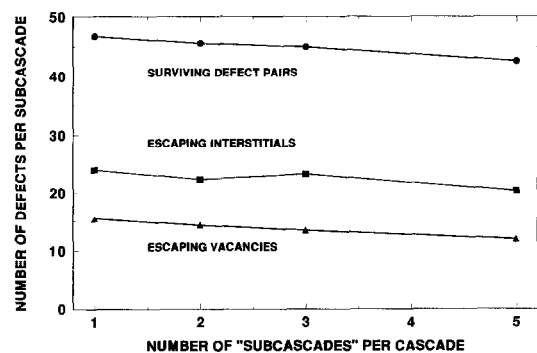


Fig. 3. The numbers of surviving defect pairs and escaping defects after annealing groups of subcascades, as in Fig. 2, at 400 K, as a function of the number of subcascades in the group.

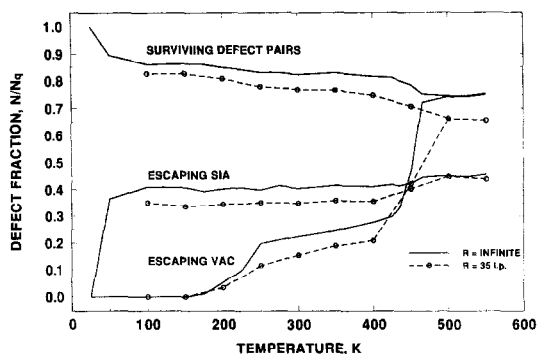


Fig. 4. A comparison of annealing results for individual 25 keV copper cascades ($R = \text{infinite}$, the same curves as Fig. 1) and sets of five 25 keV 'subcascades' having an average center-to-center separation of 35 lattice parameters ($R = 35 \text{ l.p.}$). Each data point represents the average of anneals of 100 different arrangements of the five cascades.

average of 100 anneals of the two individual 25 keV cascades (i.e., infinite separation), which is on the order of the standard deviation of the average values. Also, the remaining defects do not rearrange themselves significantly; there is essentially no effect of subcascade interaction on the average numbers or sizes of SIA and vacancy clusters. The weak interaction among defects from adjacent subcascades is further demonstrated in Fig. 5 for two cascades placed in an overlapping configuration, with a center-to-center separation of only five lattice parameters. There is slightly more recombination and fewer escaping defects. The average number and size of vacancy and SIA clusters remains essentially the same as for infinitely-spaced cascades at each temperature.

5. Approximating high energy cascades

In light of the small amount of interaction observed among subcascades, it should be possible to estimate defect production and evolution in high energy, subcascade-producing cascades by linearly extrapolating from results at cascade energies near the subcascade threshold. However, large numbers of such cascades would be needed in order to have a good basis for the extrapolation. Even though MD has been used successfully to simulate cascades near threshold energies, those simulations remain near the limit of computational capabilities, especially if a large number of representative configurations is required. Only a small number of cascades have been produced in the 15–25 keV energy range in copper, and even the two 25 keV cascades produced so far have relatively compact configurations that are not very representative of the size distribution of cascades (Fig. 6). Also, subcascades are typically produced with a distribution of sizes and with 'debris' (diffuse damage from lower energy collisions

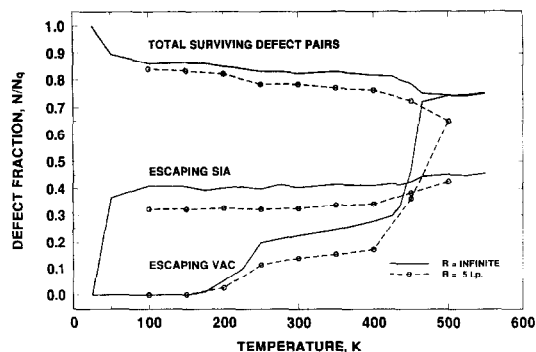


Fig. 5. The fractions of point defects surviving recombination and of vacancies and interstitials escaping from two nearly overlapped ($R = 5 \text{ l.p.}$) 25 keV cascades in copper during the annealing stage, as a function of cascade annealing temperature. The curves for infinite separation from Fig. 4 are shown for comparison.

between definable subcascades), as illustrated in Fig. 7. Thus, despite the minimal amount of interaction among defects from adjacent subcascades, the effects of cascade morphology may have significant influence on defect production at high energies and should be studied. Thus, it is of interest to develop easily-calculated approximations to high-energy cascades for such studies, especially for input to annealing simulations.

A reasonable starting point for approximating high-energy cascades is to use the binary collision approximation to simulate the collisional stage of the cascade, as in the past [10]. A major advantage over the earlier attempts is that now at least a few relatively high-energy MD simulations exist to which the binary collision calculations can be

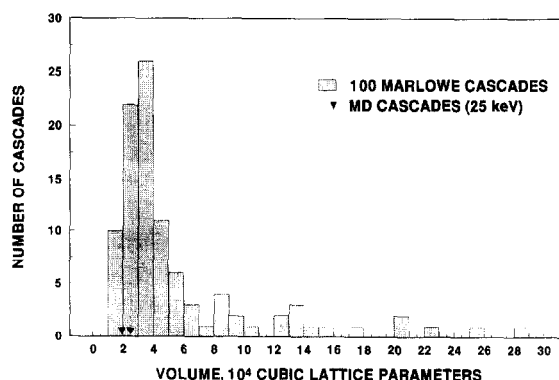


Fig. 6. The distribution of cascade sizes at the collisional stage for 30 keV cascades in copper, which have an average damage energy of 23 keV. The cascades were generated with the binary collision code MARLOWE. The volume of each cascade is measured as that of the rectangular parallelepiped oriented along the cubic crystal axes that encloses the vacant lattice sites. The volumes of the collisional stages of two 25 keV (damage energy) MD cascades, measured in the same way, are seen to be smaller than the average of this distribution.

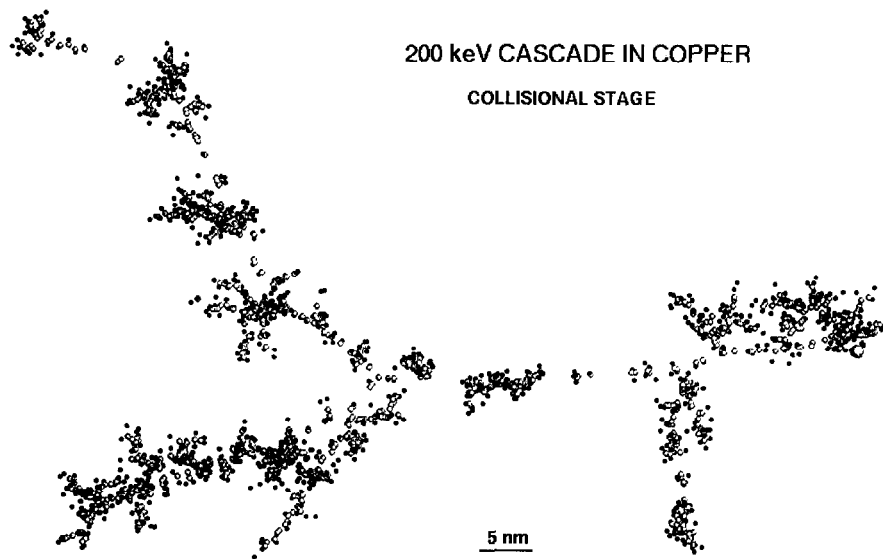


Fig. 7. The collisional stage of a 200 keV cascade in copper generated with the binary collision code MARLOWE. The lighter spheres are vacant sites and the darker spheres are displaced atoms. The primary recoil atom is shown as a larger sphere at the far right. The branches of the cascade extend into and out of the plane of the page.

calibrated. To investigate this approach, the individual time steps of the two 25 keV cascades in copper discussed above were analyzed to extract the collisional stage information, i.e., the positions of displaced atoms that would be calculated in a binary collision approximation to each cascade. Thus, both the collisional stage configuration of displaced atoms and the post-quench defect configuration are known for each of the MD cascades. The ideal MD-binary collision calibration would consist of a general algorithm for the transformation of the collisional stage displacement configuration into the quenched stage defect distribution. As a first attempt at developing such an algorithm, the method of Ref. [10] was used. That is, the atoms displaced in the collisional stage were treated as defects and placed as input into the annealing simulation, using exaggerated parameter values for defect mobility and interaction distances to simulate quenching for a simulated time of about 10 ps, the typical duration of cascade evolution through the quenching stage. Using this method, it was found possible to choose exaggerated, 'quenching', parameter values that result in correct numbers of post-quench defects, but the cluster size distributions and the compactness of the post-quench vacancy distribution observed in the MD simulations could not be achieved by this approach.

Obtaining the correct defect configuration after the artificial quenching stage may not be very important (the post-quench configuration is a transient state of the cascade process existing for a few hundred picoseconds), especially if the next step — the defect configuration following the subsequent annealing stage — can be well-described. Thus, annealing simulations were subsequently

performed on the 25 keV cascades that were artificially quenched from the collisional stage, and the results were compared to those obtained from annealing the actual quenched stage of the MD cascades. Fig. 8 shows the results as a function of annealing temperature. These results are encouraging, being qualitatively similar to those obtained for the quenched MD cascades. The largest discrepancy is in the numbers of escaping SIAs, because fewer large, immobile SIA clusters form during the artificial quench. Also, the fraction of escaping vacancies has a somewhat different temperature dependence because fewer

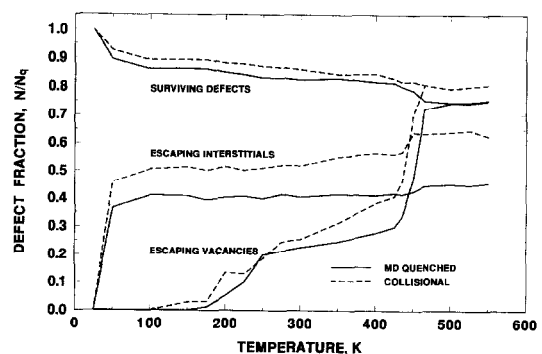


Fig. 8. The fractions of point defects surviving recombination and of vacancies and interstitials escaping from 25 keV cascades in copper during the annealing stage, as a function of cascade annealing temperature. The solid lines are for the annealing of cascades fully quenched by MD, while the dashed lines are for the annealing of the same cascades that were artificially quenched from the collisional stage.

large vacancy clusters (which give rise to the dramatic increase in escaping vacancies as they dissolve at 400–450 K) are formed during the artificial quench. Because of the importance of the number and size of SIA and vacancy clusters and their stability and diffusion characteristics to the results of the annealing stage, a more realistic artificial quenching scheme is required, especially one that more specifically deals with the energy and particle transport properties of the material.

6. Discussion

The relatively small amount of interaction among defects from adjacent subcascades during the annealing stage is due primarily to the nature of the configuration of defects in individual subcascades after the quenching stage. The formation and subsequent quenching of the thermal spike tends to concentrate the vacancies in the center of the subcascade, while the SIAs, many ejected ballistically from the cascade center, are more diffusely distributed about the periphery of the cascade region. Since the SIAs have much higher mobilities than vacancies and are at the periphery of the cascade, their probability of escaping the cascade region is much higher than their probability of interacting with the vacancies near the center. This effect is so dominating that even simple models of cascade annealing give qualitatively, and even quantitatively, similar results. Early annealing simulations of binary collision cascades subjected to a quenching recombination step were used in a study of defect interactions among closely spaced cascades that showed the interactions to be minimal [10]. A one-dimensional diffusion calculation [18] on a conceptual copper cascade having spherically symmetric defect distributions gave escaping defect fractions remarkably similar to the present results.

Even in a close grouping of subcascades, the vacancies concentrated in the center of each subcascade present a relatively small cross-section for interaction with the SIAs of any other subcascade. The consequences of the segregated spatial arrangement and the large difference in mobilities of vacancy and SIA clusters are further amplified when a significant fraction of the mobile SIA defects can move one-dimensionally. These SIA defects have a significantly smaller cross-section for interaction with other defect clusters than the single-, di- and tri-interstitials, which migrate by three-dimensional random motion. In summary, greater clustering of both vacancies and SIAs, greater compaction of the vacancy population toward the center of the cascade, and a greater fraction of glissile SIA clusters all lead to less interaction of defects among closely spaced subcascades during the annealing stage.

It is difficult to determine whether there is an effect of subcascade interaction on defect survivability and clustering during the thermal spike and quenching stages of cascade development. For example, if subcascades form in

very close proximity during the collisional stage, do their thermal spikes coalesce into a single spike of somewhat lower energy density? Any such effects would probably be unnoticed in the already wide variability in cascade features due to other effects of their random nature. The only existing MD simulations of subcascade-producing cascades are the 40 keV cascades in iron of Ref. [16]. A notable feature of these cascades is that their efficiency of defect production at the end of the quenching stage is slightly higher than predicted by extrapolation from the behavior of lower energy cascades. This may indicate that, at least, recombination is not enhanced by subcascade interaction. On the other hand, increased defect production efficiency due to the survival of defects in the debris between the major subcascades may obscure any effects of subcascade interaction.

At energies up to the subcascade threshold, the number of residual defects after the quenching stage, observed in MD simulations, increases with damage energy according to a power law [19]. At energies well into the subcascade range, where more than several subcascades are formed, the defect production should increase linearly with damage energy, since increasing the energy simply produces more damage regions that have the same defect production characteristics (the cascades of Ref. [16] fall in the transition energy range that extends somewhat above the subcascade threshold energy). Based on the results of the present annealing study of defect interactions among subcascades, linearity of defect survival with damage energy in high energy cascades should be maintained through the annealing stage of cascades as well.

Because of the importance of cluster formation within cascades in nearly every aspect of the annealing stage, it is important to be able to model the cluster sizes and their transport characteristics accurately. Although one-dimensional migration of SIA clusters has been observed in MD simulations of cascades [4,5], the mobility of small, glissile SIA clusters in copper as a function of cluster size is not well known. Thus, it is instructive to explore the sensitivity of the annealing simulations to changes in the glissile SIA cluster mobility as a function of cluster size. A study was performed to determine the sensitivity of defect survival and escape during the annealing stage to the variation of the maximum size of glissile SIA clusters in annealing simulations of two 25 keV cascades in copper [20]. Simulations were performed for models where the maximum size of glissile SIA clusters was varied from 4–20 SIAs. The results, summarized in Fig. 9, showed that all SIA clusters that are assumed to be glissile quickly escape the cascade region at virtually any temperature above 50 K. The fraction of escaping SIAs in these 25 keV copper cascades varies from 10%–80%, depending on the maximum size assumed for glissile clusters. It was also demonstrated from these results [20] that recombination during the annealing stage is due almost entirely to interaction of vacancies with the single- di- and tri-SIA clusters that

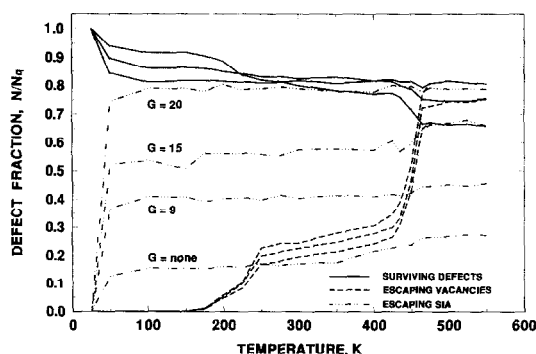


Fig. 9. The fractions of point defects surviving recombination and of vacancies and interstitials escaping from 25 keV cascades in copper during the annealing stage, as a function of cascade annealing temperature. The effects of varying the maximum size of glissile SIA clusters in the annealing model are demonstrated. The variation of the surviving defect and escaping vacancy fractions is small, but the variation of the escaping SIA fraction is dramatic. Essentially all glissile SIA clusters escape the cascade and have little interaction with the cascade vacancies.

move in three dimensions. Thus, the fraction of escaping SIAs during the annealing stage depends on both the mobility of SIA clusters as a function of size and the SIA cluster size distribution in cascades after quenching. The two 25 keV MD cascades used in these studies contain only clusters with 20 SIAs or less. If this is typical of all cascades and subcascades in copper, and if clusters of up to at least 20 SIAs are glissile, then all SIAs will always escape from each cascade. The size dependence of glissile cluster mobility should be carefully evaluated. It is expected that mobility is only weakly dependent on size in this range.

Another aspect of glissile SIA cluster transport that is not addressed in the present model is the possibility that a glissile cluster can change its glide direction either by thermal activation (with an estimated activation energy of about 0.5 eV [4,5]) or by direct interaction with another defect. Thus, the characteristics of glissile SIA cluster migration may well depend significantly on the temperature and the dose or dose rate when direction changes are frequent. When one-dimensional segments are significantly shorter than the cascade dimensions, the glissile SIA cluster will execute an effective three-dimensional random walk that will increase its probability of interaction with other defects within the cascade during the annealing stage. Thus, the characteristics of SIA loop production and mobility within cascades remains a crucial element for understanding the defect evolution during the cascade annealing stage. This phenomenon will have important consequences as well in the global picture.

Annealing simulations can also be applied directly to the global picture of cascade defect evolution by considering a large annealing volume into which MD cascades are

placed randomly in space and time to simulate actual irradiation conditions. In this way one can simulate damage accumulation under realistic temporal and spatial variations of cluster production. Thus, the annealing simulations would link the information from atomistic simulations to reaction rate theories as it determined the major input parameters for the calculation of defect accumulation transients. In addition to determining the size and number of SIA and vacancy clusters as a function of time, one could study the effects of the transformation frequency of sessile to glissile loops. It is also possible that direct comparisons of annealing simulation results can be made to experimental information, such as the dose and temperature dependence of the TEM-visible cluster density. To utilize this approach to its fullest potential, large numbers of high energy cascades need to be available for simulations. The development of an acceptably rigorous approximation to defect distributions in high energy cascades, perhaps by calibration of binary collision cascades to MD results, is clearly needed. Annealing simulations of actual irradiation conditions are in progress.

7. Conclusions

The intracascade defect interactions among a group of closely spaced cascades or subcascades are minimal, due to the segregation of the vacancy population in each cascade toward its center, as well as the vast difference in mobilities of the vacancy and SIA defects and the one-dimensional glide of glissile SIA clusters. The existence of glissile SIA clusters, formed directly in cascades, and the characteristics of their motion are extremely important elements in determining the mobile defect fractions from individual cascades and the nature of the global defect population.

Acknowledgements

This work was supported by the US Department of Energy, Office of Fusion Energy, under Contract DE-AC06-76RLO 1830, and the European Fusion Technology Programme.

References

- [1] C.H. Woo, B.N. Singh, A.A. Semenov, *J. Nucl. Mater.* 239 (1996) 7.
- [2] C.H. Woo, B.N. Singh, *Phys. Status Solidi (b)* 159 (1990) 609.
- [3] C.H. Woo, B.N. Singh, *Philos. Mag.* A65 (1992) 889.
- [4] H. Trinkaus, B.N. Singh, A.J.E. Foreman, *J. Nucl. Mater.* 199 (1992) 1.

- [5] H. Trinkaus, B.N. Singh, A.J.E. Foreman, *J. Nucl. Mater.* 206 (1993) 200.
- [6] H. Trinkaus, B.N. Singh, A.J.E. Foreman, *J. Nucl. Mater.* 212–215 (1994) 18.
- [7] B.N. Singh, S.I. Golubov, H. Trinkaus, A. Serra, Yu.N. Osetsky, A.V. Barashev, these Proceedings, p. 107.
- [8] J.R. Beeler, in: *Proc. Int. Conf. on Radiation Induced Voids in Metals*, Albany, NY, June 1971, eds. J.W. Corbett and L.C. Ianniello (1972) p. 684.
- [9] D.G. Doran, R.A. Burnett, in: *Interatomic Potentials and Simulation of Lattice Defects*, eds. P.C. Gehlen, J.R. Beeler and R.I. Jaffee (Plenum, New York, 1972) p. 403.
- [10] H.L. Heinisch, *J. Nucl. Mater.* 117 (1983) 46.
- [11] H.L. Heinisch, B.N. Singh, *J. Nucl. Mater.* 191–194 (1992) 125.
- [12] H.L. Heinisch, B.N. Singh, T. Diaz de la Rubia, *J. Nucl. Mater.* 212–215 (1994) 127.
- [13] H.L. Heinisch, *Nucl. Instrum. Meth. B102* (1995) 47.
- [14] H.L. Heinisch, B.N. Singh, *J. Nucl. Mater.* 232 (1996) 206.
- [15] T. Diaz de la Rubia, M.W. Guinan, *Mater. Sci. Forum* 97–99 (1992) 23.
- [16] R.E. Stoller, G.R. Odette, B.D. Wirth, these Proceedings, p. 49.
- [17] H.L. Heinisch, B.N. Singh, *Philos. Mag.* A67 (1993) 407.
- [18] B.N. Singh, A.J.E. Foreman, *Philos. Mag.* A66 (1992) 975.
- [19] D.J. Bacon, A.F. Calder, F. Gao, V.G. Kapinos, S.J. Wooding, *Nucl. Instrum. Meth. B102* (1995) 37.
- [20] H.L. Heinisch, in: *Proc. MRS Symp. on Microstructure Evolution During Irradiation*, MRS Fall Meeting, Dec. 1–6, 1996, in press.